

The Manipulability and Optimized Configuration of Tracked Mobile Manipulator

Pengmei Dong⁺ and Xinhua Zhao

School of Mechanical Engineering, Tianjin University of Technology, Tianjin 300384, China

The Tianjin Key Laboratory for Control Theory & Application in Complicated Systems and the School of Mechanical Engineering, Tianjin University of Technology, Tianjin 300384, China

Abstract. Based on the LeoBot-Edu-Sarm tracked mobile manipulator, first build the unified kinematics model of mobile manipulator based on generalized Jacobian matrix, then calculate the mobile manipulator, and analysis its optimized configuration, and make simulations by using Matlab. These all are the basement of the further research such as path planning and intelligent control.

Keywords: tracked mobile manipulator, 6-degree-freedom manipulator, kinematic modelling, manipulability, optimized configuration

1. Introduction

Many countries are paying more and more attention to the automation these days. It has already been used in many fields such as manufacture industry, geological exploration, archaeological science, counter-terrorism activities and so on[1]. Mobile manipulator is composed of a mobile platform and one or several manipulators. It's a complex system with the feature of nonlinear and strong coupled[2]. Common manipulator can be assorted by the mode of motion as tracked, wheeled, leg-feed mobile manipulator.

Kinematic description of mobile manipulator[3-5] reflects the kinematic relation between the articulations of manipulator and other parts of the platform[6]. It is the foundation of optimal configuration, path planning, coordination control of mobile manipulator.

This text is a disquisition on the kinematic modeling and investigation of 6-degree-freedom tracked mobile manipulator named LeoBot-Edu-Sarm. First, have data predigested, make kinematic model with Jacobian matrix, then calculate manipulability of the platform and the mobile manipulator. Then use Matlab to find out the optimized configuration and make simulations so as to analyze the locomotion of the whole system.

2. Kinematic Modelling

2.1. Mobile Platform

As shown in fig 1, it is the simplified geometrical model of the tracked mobile manipulator. Coordinate systems are set up as follows: {I}—world coordinate system, {P}—tracked mobile platform coordinate

⁺ Corresponding author . Tel.: +86-13312061517
E-mail address: dpmxinea@126.com

system. P—midpoint of two driving wheels' axis, M—joint of platform and manipulator, l_m —distance between P and M, b —distance between two driving wheels, θ_p —course angle, v_r, v_l —horizontal velocity of right, left driving wheel, θ_n —turning angle of articulation “n” ($n=1,2,\dots,6$), l_k —length of each connecting rod ($k=1,2,3,4$).

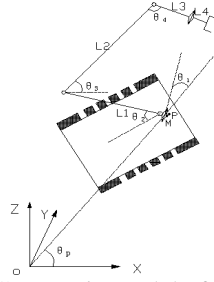


Fig. 1: Geometric model of tracked mobile manipulator

The coordinate figure of point M is that:

$$\begin{aligned} x_m &= x_p - l_m \cos \theta_p \\ y_m &= y_p - l_m \sin \theta_p \\ z_m &= 0 \end{aligned} \quad (1)$$

Calculate the derivation of (1):

$$\begin{bmatrix} \dot{x}_m \\ \dot{y}_m \\ \dot{\theta}_p \end{bmatrix} = \begin{bmatrix} \frac{\cos \theta_p}{2} + \frac{l_m \sin \theta_p}{b} & \frac{\cos \theta_p}{2} - \frac{l_m \sin \theta_p}{b} \\ \frac{\sin \theta_p}{2} - \frac{l_m \cos \theta_p}{b} & \frac{\sin \theta_p}{2} + \frac{l_m \cos \theta_p}{b} \\ \frac{1}{b} & -\frac{1}{b} \end{bmatrix} \begin{bmatrix} v_r \\ v_l \end{bmatrix} \quad (2)$$

The angular velocity of point P is $\omega_p = \dot{\theta}_p = \frac{v_r - v_l}{b}$ (3)

The velocity of point P can be represented by the horizontal velocity of two driving wheels:

$$v_p = \frac{1}{2}(v_r + v_l) \quad (4)$$

As the velocity of P is perpendicular to wheel axle, it's components in the world coordinate system are

$$\dot{x}_p = v_{px} = v_p \cos \theta_p, \quad \dot{y}_p = v_{py} = v_p \sin \theta_p, \quad \dot{z}_p = 0 \quad (5)$$

Collate (5) by the expunction of v_p : $\dot{x}_p \sin \theta_p - \dot{y}_p \cos \theta_p = 0$ (6)

It is the constraint equation of the platform.

As the platform is differentiating controlled by left and right wheels, choose v_r and v_l as controlling input variables, and the platform has three variables — x_p, y_p and θ_p . So the degrees of freedom are more than the number of drivers. This is one of the characteristics of incomplete inhibited system.

Ensure that you return to the ‘Els-body-text’ style, the style that you will mainly be using for large blocks of text, when you have completed your bulleted list.

2.2. End Effector

The coordinate figure of point E (End Effector) is that:

$$\begin{aligned} x_e &= x_m - l_1 \cos \theta_2 \cos(\theta_1 + \theta_p) + l_2 \cos(\theta_2 + \theta_3) \cos(\theta_1 + \theta_p) + \\ &\quad (l_3 + l_4) \cos(\theta_2 + \theta_3 + \theta_4) \cos(\theta_1 + \theta_p) \\ y_e &= y_m - l_1 \cos \theta_2 \sin(\theta_1 + \theta_p) + l_2 \cos(\theta_2 + \theta_3) \sin(\theta_1 + \theta_p) + \\ &\quad (l_3 + l_4) \cos(\theta_2 + \theta_3 + \theta_4) \sin(\theta_1 + \theta_p) \\ z_e &= z_m + l_1 \sin \theta_2 + l_2 \sin(\theta_2 + \theta_3) - l_3 \sin(\theta_2 + \theta_3 + \theta_4) \end{aligned} \quad (7)$$

Calculate the derivation of (7):

$$\begin{bmatrix} \dot{x}_e \\ \dot{y}_e \end{bmatrix} = \begin{bmatrix} \dot{x}_m \\ \dot{y}_m \end{bmatrix} + \begin{bmatrix} J_{11} & J_{12} & J_{13} & J_{14} \\ J_{21} & J_{22} & J_{23} & J_{24} \end{bmatrix} \begin{bmatrix} \dot{\theta}_1 + \dot{\theta}_p \\ \dot{\theta}_2 \\ \dot{\theta}_3 \\ \dot{\theta}_4 \end{bmatrix} \quad (8)$$

$$\dot{z}_e = \dot{z}_m + \begin{bmatrix} 0 & B_{12} & B_{13} & B_{14} \end{bmatrix} \begin{bmatrix} \dot{\theta}_1 + \dot{\theta}_p \\ \dot{\theta}_2 \\ \dot{\theta}_3 \\ \dot{\theta}_4 \end{bmatrix} \quad (9)$$

Besides:

$$B_{12} = l_1 \cos \theta_2 + l_2 \cos(\theta_2 + \theta_3) - (l_3 + l_4) \cos(\theta_2 + \theta_3 + \theta_4)$$

$$B_{13} = l_2 \cos(\theta_2 + \theta_3) - (l_3 + l_4) \cos(\theta_2 + \theta_3 + \theta_4)$$

$$B_{14} = -(l_3 + l_4) \cos(\theta_2 + \theta_3 + \theta_4)$$

And (8) can be also written as (10):

$$\begin{bmatrix} \dot{x}_e \\ \dot{y}_e \end{bmatrix} = \begin{bmatrix} \dot{x}_m \\ \dot{y}_m \end{bmatrix} + \begin{bmatrix} \cos \theta_p & -\sin \theta_p \\ \sin \theta_p & \cos \theta_p \end{bmatrix} \begin{bmatrix} Q_{11} & Q_{12} & Q_{13} & Q_{14} \\ Q_{21} & Q_{22} & Q_{23} & Q_{24} \end{bmatrix} \begin{bmatrix} \dot{\theta}_1 + \dot{\theta}_p \\ \dot{\theta}_2 \\ \dot{\theta}_3 \\ \dot{\theta}_4 \end{bmatrix} \quad (10)$$

$$Q_{11} = \sin \theta [l_1 \cos \theta_2 - l_2 \cos(\theta_2 + \theta_3) - (l_3 + l_4) \cos(\theta_2 + \theta_3 + \theta_4)]$$

$$Q_{12} = \cos \theta [l_1 \sin \theta_2 - l_2 \sin(\theta_2 + \theta_3) - (l_3 + l_4) \sin(\theta_2 + \theta_3 + \theta_4)]$$

$$Q_{13} = -\cos \theta [l_2 \sin(\theta_2 + \theta_3) + (l_3 + l_4) \sin(\theta_2 + \theta_3 + \theta_4)]$$

$$Q_{14} = -\cos \theta [(l_3 + l_4) \sin(\theta_2 + \theta_3 + \theta_4)]$$

$$Q_{21} = -\cos \theta [l_1 \cos \theta_2 - l_2 \cos(\theta_2 + \theta_3) - (l_3 + l_4) \cos(\theta_2 + \theta_3 + \theta_4)]$$

$$Q_{22} = \sin \theta [l_1 \sin \theta_2 - l_2 \sin(\theta_2 + \theta_3) - (l_3 + l_4) \sin(\theta_2 + \theta_3 + \theta_4)]$$

$$Q_{23} = -\sin \theta [l_2 \sin(\theta_2 + \theta_3) + (l_3 + l_4) \sin(\theta_2 + \theta_3 + \theta_4)]$$

$$Q_{24} = -\sin \theta [(l_3 + l_4) \sin(\theta_2 + \theta_3 + \theta_4)]$$

Integrate (4) (9) (10), it can educe the connection among the end effector, the horizontal velocity of two driving wheels and turning angle of the articulations of manipulator:

$$\begin{bmatrix} \dot{x}_e \\ \dot{y}_e \\ \dot{z}_e \end{bmatrix} = J_2 * \phi \quad J_2 = \begin{bmatrix} A_{11} & A_{12} & A_{13} & A_{14} & A_{15} & A_{16} \\ A_{21} & A_{22} & A_{23} & A_{24} & A_{25} & A_{26} \\ 0 & 0 & 0 & A_{34} & A_{35} & A_{36} \end{bmatrix} \quad (11)$$

Besides:

$$A_{11} = \cos \theta_p \left(\frac{1}{2} + \frac{1}{b} Q_{11} \right) + \frac{1}{b} \sin \theta_p (l_m - Q_{21})$$

$$A_{12} = \cos \theta_p \left(\frac{1}{2} - \frac{1}{b} Q_{11} \right) - \frac{1}{b} \sin \theta_p (l_m - Q_{21})$$

$$A_{13} = \cos \theta_p * Q_{11} - \sin \theta_p * Q_{21}$$

$$A_{14} = \cos \theta_p * Q_{12} - \sin \theta_p * Q_{22}$$

$$A_{15} = \cos \theta_p * Q_{13} - \sin \theta_p * Q_{23}$$

$$A_{16} = \cos \theta_p * Q_{14} - \sin \theta_p * Q_{24}$$

$$A_{21} = \sin \theta_p \left(\frac{1}{2} + \frac{1}{b} Q_{11} \right) - \frac{1}{b} \cos \theta_p (l_m - Q_{21})$$

$$A_{22} = \sin \theta_p \left(\frac{1}{2} - \frac{1}{b} Q_{11} \right) + \frac{1}{b} \cos \theta_p (l_m - Q_{21})$$

$$A_{23} = \sin \theta_p * Q_{11} + \cos \theta_p * Q_{21}$$

$$A_{24} = \sin \theta_p * Q_{12} + \cos \theta_p * Q_{22}$$

$$A_{25} = \sin \theta_p * Q_{13} + \cos \theta_p * Q_{23}$$

$$A_{26} = \sin \theta_p * Q_{14} + \cos \theta_p * Q_{24}$$

$$A_{34} = l_1 \cos \theta_2 + l_2 \cos(\theta_2 + \theta_3) - (l_3 + l_4) \cos(\theta_2 + \theta_3 + \theta_4)$$

$$A_{35} = l_2 \cos(\theta_2 + \theta_3) - (l_3 + l_4) \cos(\theta_2 + \theta_3 + \theta_4)$$

$$A_{36} = -(l_3 + l_4) \cos(\theta_2 + \theta_3 + \theta_4)$$

And J_2 in (11) is the generalized Jacobian matrix of tracked mobile manipulator. It indicates the relationship among end effector, locality of manipulator fixed on the platform, the angular velocity of the articulations and the horizontal velocity of two pedrails.

3. Manipulability and Optimized Configuration of Mobile Manipulator

The operability of a robot depends on the locomotive capability along all the directions freely in the working space. It can be considered from two parts:

- 1) The capability of reaching a certain or a series of positions.
- 2) The capability of changing positions and gestures while some certain parameters are already known.

3.1. Manipulability of Mobile Platform

While the velocity of point E in plane xoy can be represented by v_r and v_l as:

$$\begin{bmatrix} \dot{x}_e \\ \dot{y}_e \end{bmatrix} = \begin{bmatrix} \cos \theta_p & -\sin \theta_p \\ \sin \theta_p & \cos \theta_p \end{bmatrix} \begin{bmatrix} \frac{1}{2} + \frac{1}{b} Q_{11} & \frac{1}{2} - \frac{1}{b} Q_{11} \\ -\frac{l_m}{b} + \frac{1}{b} Q_{21} & \frac{l_m}{b} - \frac{1}{b} Q_{21} \end{bmatrix} \begin{bmatrix} v_r \\ v_l \end{bmatrix} \quad (12)$$

Its' abbreviation is $\dot{P}_e = J_1^* q^1$. So the manipulability of mobile platform[7] is $\det|J_1 J_1^T|$. It shows how the movement of platform affects on the end effector. and the ability to change it.

$$\begin{aligned} \det|J_1 J_1^T| &= (\sin^2 \theta_p + \cos^2 \theta_p) * \frac{1}{b^2} (l_m - Q_{21})^2 \\ &= \frac{1}{b^2} [l_m + l_1 \cos \theta_1 \cos \theta_2 - l_2 \cos \theta_1 \cos(\theta_2 + \theta_3) - (l_3 + l_4) \cos \theta_1 \cos(\theta_2 + \theta_3 + \theta_4)] \end{aligned} \quad (13)$$

From (13) above we can see that the manipulability of platform is only related to the locality of manipulator fixed on the platform and the turning angles of the first four articulations, and it has nothing to do with course angle θ_p .

As point M is on axis xp, when the distance between P and M is limited and can be ignored, $\det|J_1 J_1^T|$ can be approximated as (14):

$$\det|J_1 J_1^T| = \frac{1}{b^2} [l_1 \cos \theta_1 \cos \theta_2 - l_2 \cos \theta_1 \cos(\theta_2 + \theta_3) - (l_3 + l_4) \cos \theta_1 \cos(\theta_2 + \theta_3 + \theta_4)] \quad (14)$$

It is inferred from (14) that manipulability of platform gets to maximum while $\theta_1 = 0^\circ$.

When $\det|J_1 J_1^T| = 0$, manipulator exhibits singular configuration. Considering the effective turning angle of each articulation, singular configuration of the manipulator appears in these situations below:

$$\textcircled{1} \theta_1 = \pm \frac{\pi}{2}$$

$$\textcircled{2} \theta_2 = \frac{\pi}{2}, \text{ and } \theta_3 = 0 \text{ or } \theta_3 = \pm\pi, \text{ and } \theta_4 = 0 \text{ or } \theta_4 = \pm\pi$$

At the same time, the locomotion of platform has no contribution to the locomotion of manipulator on plane 'xoy'. So we should avoid these in practice.

3.2. Manipulability and optimized configuration of Mobile Manipulator

Manipulability of mobile manipulator is defined as $\det|J_2 J_2^T|$,

$$\det|J_2 J_2^T| = \begin{vmatrix} \begin{bmatrix} A_{11} & A_{12} & A_{13} & A_{14} & A_{15} & A_{16} \\ A_{21} & A_{22} & A_{23} & A_{24} & A_{25} & A_{26} \\ 0 & 0 & 0 & A_{34} & A_{35} & A_{36} \end{bmatrix} & \begin{bmatrix} A_{11} & A_{21} & 0 \\ A_{12} & A_{22} & 0 \\ A_{13} & A_{23} & 0 \\ A_{14} & A_{24} & A_{34} \\ A_{15} & A_{25} & A_{35} \\ A_{16} & A_{26} & A_{36} \end{bmatrix} \end{vmatrix} \quad (15)$$

Analysis of the result of (15) indicates manipulability of mobile manipulator is irrelevant to the course angle θ_p . Choose θ_2, θ_3 and θ_4 as variables, seek for the optimized configuration of the manipulator and simulate it with Matlab.

On the assumption that each articulation moves constantly, the relation among θ_2, θ_3 and θ_4 is can be seen in fig (2). The connections between turning angle of the articulations and the manipulator are shown in the next 3 parts:

① As shown in fig (3), suppose θ_2, θ_3 change within limits, while $\theta_4 = 27.01369^\circ$, the manipulability of mobile manipulator reaches maximum. Meanwhile, $\theta_2 = 114.18535^\circ, \theta_3 = 40.52064^\circ$. As θ_4 gets larger, manipulability increases at first, and reduced after θ_4 reaching 27.01369° .

② As shown in fig (4), suppose θ_2, θ_4 change within limits, while $\theta_3 = 198.10043^\circ$, the manipulability of mobile manipulator reaches maximum. Meanwhile, $\theta_2 = 15.00764^\circ, \theta_4 = 40.52064^\circ$. As θ_3 gets larger, manipulability increases at first, and reduced after θ_3 reaching 198.10043° .

③As shown in fig (5), suppose θ_3 、 θ_4 change within limits , while $\theta_2 = 22.51146^\circ$, the manipulability of mobile manipulator reaches maximum. Meanwhile, $\theta_3 = 198.10318^\circ$, $\theta_4 = 199.59936^\circ$.As θ_2 gets larger, manipulability increases at first, and reduced after θ_2 reaching 22.51146° .

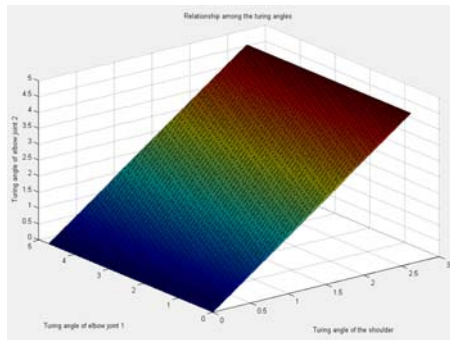


Fig. 2: Relationship among the turning angles

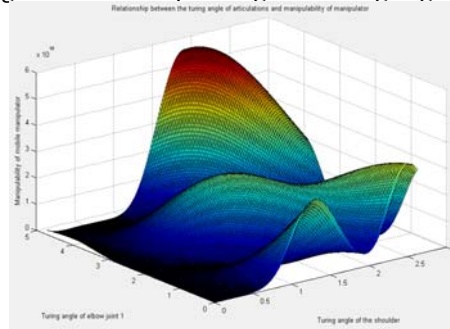


Fig.3: Relationship among turning angle of the shoulder and elbow joint 1 and manipulability of manipulator

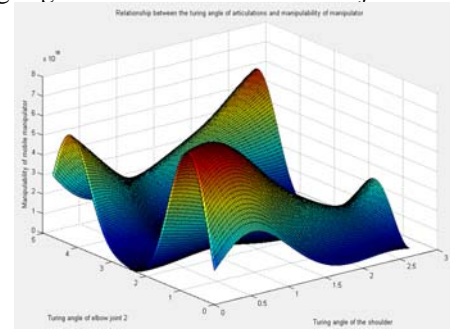


Fig.4: Relationship among turning angle of the shoulder and elbow joint 2 and manipulability of manipulator

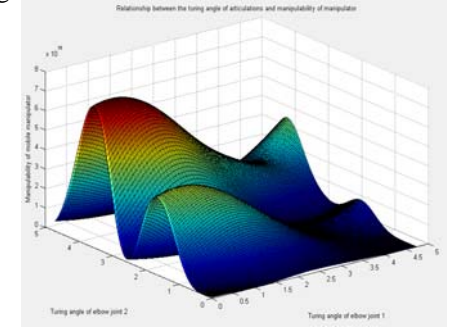


Fig.5: Relationship among turning angle of elbow joint 1 and elbow joint 2 and manipulability of manipulator

4. Conclusion

This paper is about the unified kinematics model of tracked mobile manipulator, then calculate the manipulability of the platform and the mobile manipulator. And the conclusion is that both of the two are not relevant to θ_p . So we must try to avert these singular configurations in motion controlling in practice to ensure the manipulation correctly. At last, simulation is made with Matlab to analysis the optimized configuration. These all are the basement of the further research such as path planning and intelligent control.

5. Acknowledgements

The author gratefully acknowledges the support of the National Natural Science Foundation of P.R. China under Grant No.50675156, the National High-tech R&D Program(863 Program) of P.R. China under Grant No.2007AA04Z203, and Tianjin Natural Science Foundation of P.R. of China under Grant No.10JCZDJC22900.

6. References

- [1] N. Li, X.H. Zhao. Mobile Manipulator Kinematics Model and Manipulability Measure. Journal of Tianjin University of Technology, 2006, 22(6): 39-43
- [2] X.C. Li, J.Q. Yi. Path Planning Simulation for Mobile Manipulators Based on OpenGL. Journal of System Simulation, 2006, 18(1): 196-199
- [3] C.A.Liu, H. Zhou. Path Planning of Differential Wheeled Mobile Manipulator. Journal of Astronautics,2004, 25(2):183-186
- [4] B.Bayle. Kinematic Modelling of Wheeled Mobile Manipulators. Proceedins of the 2003 IEEE international Conference on Robotics and Automation, 2003, 69-74
- [5] Seraji.Motion Control of Mobile Manipulators.Proceedings of the 1993IEEE/RSJ International Conference on Intelligent Robots and Systems Yokohama, 1993 , P:2056-2063,1993.
- [6] T.S.Wang. Kinematics and Dynamics of Robots. Xi'an University of Science and Technology Press, 1990
- [7] S.S. Zhang, D.T. Yu. Optimized Configuration of Wheeled Mobile Manipulator. Journal of Beijing University of Science and Technology, 2000, 22(6): 565-568